

The dynamics of coupled populations subject to control

Stephanie J. Peacock · Andrew W. Bateman · Martin

Krkošek · Mark A. Lewis

Received: date / Accepted: date

1 **Abstract** The dynamics of coupled populations have mostly been studied in the context of metapopulation
2 viability with application to, for example, species at risk. However, when considering pests and pathogens,
3 eradication, not persistence, is often the end goal. Humans may intervene to control nuisance populations, re-
4 sulting in reciprocal interactions between the human and natural systems that can lead to unexpected dynamics.
5 The incidence of these human-natural couplings has been increasing, hastening the need to better understand
6 the emergent properties of such systems in order to predict and manage outbreaks of pests and pathogens. For
7 example, the success of the growing aquaculture industry depends on our ability to manage pathogens and
8 maintain a healthy environment for farmed and wild fish. We developed a model for the dynamics of con-
9 nected populations subject to control, motivated by sea louse parasites that can disperse among salmon farms.
10 The model includes exponential population growth with a forced decline when populations reach a thresh-

S.J. Peacock
Biological Sciences, University of Alberta, Edmonton, Alberta, Canada T6G 2E9
Tel.: 1 778 266 0575
Fax: 1 780 492 8373
E-mail: stephanie.peacock@ualberta.ca

A.W. Bateman
Ecology and Evolutionary Biology, University of Toronto, Toronto, Ontario, Canada M5S 3B2
Mathematical and Statistical Sciences, University of Alberta, Edmonton, Alberta, Canada T6G 2G1
Salmon Coast Field Station, Simoom Sound, British Columbia, Canada V0P 1S0

M. Krkošek
Ecology and Evolutionary Biology, University of Toronto, Toronto, Ontario, Canada M5S 3B2
Salmon Coast Field Station, Simoom Sound, British Columbia, Canada V0P 1S0

M.A. Lewis
Biological Sciences, University of Alberta, Edmonton, Alberta, Canada T6G 2E9
Mathematical and Statistical Sciences, University of Alberta, Edmonton, Alberta, Canada T6G 2G1

11 old, representing control interventions. Coupling two populations with equal growth rates resulted in phase
12 locking or synchrony in their dynamics. Populations with different growth rates had different periods of oscil-
13 lation, leading to quasiperiodic dynamics when coupled. Adding small amounts of stochasticity destabilized
14 quasiperiodic cycles to chaos, while stochasticity was damped for periodic or stable dynamics. Our analysis
15 suggests that strict treatment thresholds, although well intended, can complicate parasite dynamics and hinder
16 control efforts. Synchronizing populations via coordinated management among farms leads to more effective
17 control that is required less frequently. Our model is simple and generally applicable to other systems where
18 dispersal affects the management of pests and pathogens.

19 **Keywords** aquaculture, dispersal, ecosystem service, phase locking, population dynamics, synchrony

20 **1 Introduction**

21 As the global human population grows, there is an increasing need to understand how interactions between
22 human and natural systems alter ecosystems and the services they provide (Millennium Ecosystem Assessment
23 2005). Social and ecological systems have traditionally been studied separately, but their integration as coupled
24 human and natural systems (CHANS) can reveal unexpected dynamics due to nonlinearities and thresholds
25 in the way that humans and ecosystems interact (Liu et al 2007). CHANS can exhibit emergent properties,
26 not present in isolated human or natural systems but resulting from the interactions between them. There
27 is a need to integrate studies of human actions with the natural dynamics of populations and communities
28 to understand relevant feedbacks and develop effective policy that reduces human degradation of essential
29 ecosystems services.

30 The natural dynamics of pests and pathogens have been of interest to scientists for some time, due to the
31 economic importance of agricultural pests (Oerke 2006) and human cost of transmissible diseases (Keeling
32 and Gilligan 2000, e.g.). The role of dispersal among populations in hindering control efforts has long been
33 recognized (Levins 1969, e.g.). Theoretical models of coupled populations have shown that if neighbouring
34 populations fluctuate out of phase, such that high abundances at one location correspond to low abundances at

35 another, dispersal can increase the probability of persistence via the rescue effect (Brown and Kodric-Brown
36 1977; Kendall and Fox 1998). The rescue effect is often thought of as beneficial in the context of population
37 viability of endangered species, but in the context of disease, dispersal among local populations with asyn-
38 chronous dynamics may hinder efforts to eradicate disease (e.g., Bolker and Grenfell 1996). Mathematical
39 models (e.g., Liebhold et al 2004; Holt and McPeck 1996; Hastings 1993) and observational data (e.g., Ranta
40 et al 1995; Steen et al 1996) have suggested that dispersal will tend to synchronize local populations. Syn-
41 chronized populations are more susceptible to extinction because stochastic events or human intervention can
42 cause catastrophic losses when all populations are at low abundance, with little opportunity for recolonization.
43 Paradoxically, dispersal could therefore help or hinder efforts to control disease in metapopulations depending
44 on whether dispersal results in synchronized pathogen dynamics, or the rescue effect (Abbott 2011).

45 Treatments with chemotherapeutants and wildlife culls (e.g., to reduce disease transmission) are examples
46 of control efforts that result in an immediate decline in the unwanted populations, but resurgence may be swift
47 if nearby populations persist. The optimal allocation of control effort among subpopulations may depend on
48 the level of connectivity and relative growth rates of the populations. For example, in control of the yellow
49 legged herring gull, a nuisance species in the western Mediterranean, the magnitude of the cull and life stage
50 to be targeted depends on the dispersal rate (and relative growth rates) among gull populations (Brooks and
51 Lebreton 2001). Tuberculosis in New Zealand possums can be controlled by culling infected individuals with
52 poison baits, but the effectiveness of this control depends on the timing of application and spatial configuration
53 of habitat patches (Fulford et al 2002). In general, asynchrony in the dynamics of disease among host local
54 populations likely decreases the probability of successful eradication (Earn et al 1998). Indeed, it has been
55 proposed that efforts to eradicate measles on a global scale were hampered after vaccination programs of the
56 late-1960s inadvertently resulted in the decorrelation of measles epidemics in UK cities (Bolker and Grenfell
57 1996).

58 The motivation for this study came from parasite dynamics in open-net aquaculture; a coupled human and
59 natural system where the eradication of pathogens has proved difficult. The rapid expansion of aquaculture
60 (FAO 2014) has resulted in changes to coastal ecosystems including the emergence of disease (Walker and

61 Winton 2010) and transmission of pathogens between farmed and wild fish (Heggberget et al 1993). In regions
62 where farmed and wild fish coexist, the health of the system depends on effective management of disease
63 in farmed fish (Peacock et al 2013; Tompkins et al 2015). Connectivity among populations in the marine
64 environment is typically higher than in terrestrial systems (McCallum et al 2003), and dispersal of pathogens
65 among host populations can complicate disease control.

66 In particular, parasitic copepods known as sea lice or salmon lice, predominantly *Lepeophtheirus salmonis*
67 and *Caligus* spp., have been a persistent problem in salmon aquaculture, costing millions of dollars in treat-
68 ment and reduced feed conversion ratios, negatively impacting fish health, and damaging public perception of
69 farmed salmon (Costello 2009). Many approaches have been taken to minimize sea louse outbreaks, includ-
70 ing biomass restrictions to limit host density, strategic siting of farms, the use of cleaner fish that prey on sea
71 lice, and the application of chemotherapeutants (Rae 2002; Brooks 2009). Sea louse populations on salmon
72 farms within a region are connected via the dispersal of free-living larvae (Adams et al 2012), and studies have
73 shown that critical host density thresholds for sea lice exist at regional scales (Frazer et al 2012; Jansen et al
74 2012; Kristoffersen et al 2013). It has been estimated that 28% of infections are due to the influx of larvae
75 from neighbouring farms (Aldrin et al 2013). This connectivity among farms affects the growth of sea louse
76 populations on any given farm and the efficacy of treatments. Furthermore, frequent and less effective use of
77 chemotherapeutants may facilitate the evolution of resistance in sea lice (Aaen et al 2015), which is a major
78 challenge facing the aquaculture industry (Igboeli et al 2014). Coordination of management among farms may
79 be key in effectively managing sea lice (Kristoffersen et al 2013), as well as the spread of other pathogens.
80 Many studies have focused on statistical analyses of monitoring data to uncover the relationships among farms
81 (e.g., Jansen et al 2012; Aldrin et al 2013; Rogers et al 2013; Revie et al 2002) but much can be learned from
82 applying more general theoretical models of population and disease dynamics (e.g., Frazer et al 2012).

83 In this paper, we develop a simple model for the dynamics of two populations connected by dispersal, where
84 each population is subject to external control when it reaches a threshold density. The model complements
85 previous work examining sea louse populations on individual salmon farms (Krkošek et al 2010; Rogers et al
86 2013) and within a region (Jansen et al 2012; Aldrin et al 2013) to explicitly examine how connectivity between

87 parasite populations on adjacent farms can alter the timing and frequency of treatments. This work also builds
 88 on our general theoretical understanding of how dispersal (Hastings 1993; Goldwyn and Hastings 2011; Dey
 89 et al 2015; Kendall and Fox 1998) and intervention (Chau 2000; Sah et al 2013) affect the dynamics of coupled
 90 populations. The model was motivated by sea lice on farmed salmon, but has general applicability to other
 91 systems where dispersal affects control, such as in agricultural pests of crops within a region (Ives and Settle
 92 1997), and transmissible diseases in wildlife (Tompkins et al 2015) and humans (e.g., Bolker and Grenfell
 93 1996).

94 2 Methods

95 2.1 A simple model for growth and control

96 Analyses of sea louse population dynamics on isolated salmon farms suggest that parasite populations grow
 97 exponentially in the absence of treatment (Krkošek et al 2010; Rogers et al 2013). Exponential growth is not
 98 unique to sea lice, and has been observed in birds (Van Bael and Pruett-Jones 1996), mammals (Silva 2003), and
 99 insects (Birch 1948), and has been used to describe dynamics of other agricultural pests (e.g., Samways 1979).
 100 Although negative density dependence will regulate populations at some point, management intervention in
 101 the case of pests and parasites may prevent populations from reaching such high densities. Thus, although
 102 the following model was motivated by sea louse parasites on salmon farms, it likely has broad applicability
 103 and may inform management of other pests and parasites. In developing the model, we refer to populations in
 104 adjacent patches rather than parasites on adjacent salmon farms to maintain this generality.

105 The dynamics of two populations that are continuously coupled by dispersal are described by,

$$\begin{bmatrix} u \\ v \end{bmatrix}' = \begin{bmatrix} r_{uu} & r_{uv} \\ r_{vu} & r_{vv} \end{bmatrix} \begin{bmatrix} u \\ v \end{bmatrix}, \quad (1)$$

106 where u is the population density in patch one, v is the population density in patch two, r_{ii} is the internal growth
 107 rate of population i where $i = u$ or v and r_{ij} is the connectivity probability from population j to population i .

108 We refer to the total growth rate of population $i = u$ or v as the row sum of internal growth and connectivity:
 109 $r_{ii} + r_{ij}$. The solutions for $u(t) = f_u(t, u_0, v_0)$ and $v(t) = f_v(t, u_0, v_0)$ are given in Appendix A.

110 We included control treatments by forcing a reduction in a population when it reached the threshold abun-
 111 dance of N_{\max} . Many countries, including Norway, Ireland, the United States, and Canada, require salmon
 112 farms to treat their fish with chemotherapeutants when a threshold sea louse abundance is reached, but this
 113 threshold may vary among regions (Brooks 2009). For our simulations, we chose $N_{\max} = 3$ motile lice per
 114 fish, based on guidelines in Pacific Canada that recommend treatment when farmed salmon have an average of
 115 three lice per fish (British Columbia Ministry of Agriculture and Lands 2005), but the value of the threshold is
 116 arbitrary for the qualitative analysis we perform here. Observations suggest that chemotherapeutants may kill
 117 up to 95% of motile sea lice on treated farmed salmon (Lees et al 2008), although treatment efficacy may be
 118 lower in many regions and is undoubtedly changing (Aaen et al 2015). We assumed that treatments were ef-
 119 fective, and when either $u(t)$ or $v(t)$ exceeded N_{\max} , we modelled a treatment of that population by forcing the
 120 dynamics to reset with the initial condition for the treated population being a 95% reduction from the threshold
 121 (i.e., $N_{\min} = (1 - 0.95)N_{\max}$), and the initial condition for the untreated population being equal to the density
 122 prior to treatment of the other population. For example, starting with initial population densities u_k and v_k at
 123 $t = 0$, if $u(t)$ reaches the threshold N_{\max} at time $t = T_u$, the system would be reset with $t = 0$ and initial
 124 conditions $u_{k+1} = N_{\min}$ and $v_{k+1} = f_v(T_u, u_k, v_k)$. The subscript k here represents the treatment number
 125 counted across both populations. In the following section, we develop a discrete-time model that describes the
 126 population density at treatment $k + 1$ based on the population density at treatment k .

127 2.2 Discrete-time treatment dynamics

128 We aimed to understand the conditions under which the populations will become synchronized, settle into a
 129 regular pattern of alternating treatments, or have unpredictable treatment timing. To this end, we reduced the
 130 dimensionality of the system while retaining key properties (Schaffer 1985) by deriving a discrete-time map
 131 for the population density in a focal population when the other population is treated. This approach is related

132 to “peak to peak” dynamics of time series data in which past maxima are used to predict future peaks in time-
 133 series oscillations (e.g., Rinaldi et al 2001). A similar approach is also often used to reduce the dimensionality
 134 of a system of three or more differential equations by plotting successive points where the three-dimensional
 135 phase dynamics pass through a two-dimensional plane, called a Poincaré section (e.g., Hastings and Powell
 136 1991; Schaffer 1985).

137 Given the initial population densities in the two patches, we solved Eq. (1) for the time, T_u , until population
 138 u reaches the treatment threshold (Appendix A) and the time, T_v , until population v reaches the treatment
 139 threshold. We calculated $\tilde{T} = T_u - T_v$, where $\tilde{T} < 0$ indicates that the treatment of u will happen next, and
 140 $\tilde{T} > 0$ indicates that the treatment of v will happen next. The population densities after the next treatment $k + 1$
 141 are therefore

$$\begin{bmatrix} u \\ v \end{bmatrix}_{k+1} = \underbrace{(1 - H(\tilde{T})) \begin{bmatrix} N_{\min} \\ f_v(T_u, u_k, v_k) \end{bmatrix}}_{u \text{ is treated}} + \underbrace{H(\tilde{T}) \begin{bmatrix} f_u(T_v, u_k, v_k) \\ N_{\min} \end{bmatrix}}_{v \text{ is treated}}, \quad (2)$$

142 where $H(\tilde{T})$ is the Heaviside step function that equals zero when $\tilde{T} < 0$ and one otherwise. We used the
 143 dynamical system described by (2) to construct a return map that takes the u when v is initially treated, u^* ,
 144 and returns u the next time v is treated, $\phi(u^*)$. We refer to $\phi(u^*)$ as the population density (in patch one) at
 145 re-treatment (of patch two). We show in Appendix B that the general equation for this return map is

$$\phi(u^*) = \underbrace{H(\tilde{T}_0) f_u(T_{v0}, u^*, N_{\min})}_{m=0} + \underbrace{\left[\sum_{m=1}^{\infty} H(\tilde{T}_m) \prod_{n=0}^{m-1} [1 - H(\tilde{T}_n)] \right] f_u(T_{vm}, N_{\min}, v_{m-1})}_{m \geq 1}, \quad (3)$$

146 where treatment of u occurs m times before v is treated again. The time between treatment $m - 1$ and the next
 147 treatment of v is denoted T_{vm} , and $\tilde{T}_m = T_{um} - T_{vm}$. The value of m depends on the relative growth rates
 148 of the two populations and the magnitude of connectivity. The values of T_{um} and T_{vm} cannot be solved for
 149 explicitly (Appendix A), therefore we simulated the dynamics using a recursive algorithm to obtain the shape
 150 of $\phi(u^*)$ (Appendix C).

Table 1 Summary of scenarios for how increasing connectivity affects dynamics.

Scenario	Growth rates			
	<i>u</i> internal	<i>v</i> internal	from <i>u</i> to <i>v</i>	from <i>v</i> to <i>u</i>
	r_{uu}	r_{vv}	r_{vu}	r_{uv}
A	1.00	1.00	0.01 → 1.00*	0.01 → 1.00*
B	1.00	1.00	0.01 → 1.00	0.01
C	1.00	0.50	0.01 → 1.00	0.01 → 1.00
D	1.00	0.50	0.01 → 1.00	0.01

*Under scenario A, we considered connectivity increasing to 2.00 when assessing the frequency of treatments.

151 2.3 Parameter sensitivity

152 We investigated the dynamics of the return map for a limited number of parameter combinations with each
 153 growth rate constrained between zero and two. A comprehensive description of the dynamics of the return
 154 map under all parameter combinations was impossible because the return map had to be simulated, so we
 155 focused on results from four scenarios that describe parameter changes that might occur in networks of salmon
 156 farms (Table 1). First, we considered a scenario where the internal growth rates were constant and equal at
 157 $r_{uu} = r_{vv} = 1.00$ and connectivity increased from 0.01 to 1.00 in increments of 0.01 ($r_{uv} = r_{vu} = r_{ij}$,
 158 scenario A). This scenario could represent two salmon farms being brought closer together, increasing exchange
 159 of parasites between them. Second, we considered increasing r_{vu} from 0.01 to 1.00, but connectivity in the
 160 other direction constant at $r_{uv} = 0.01$ (scenario B). This scenario could represent an increase in the advection
 161 of larvae from one farm to another. The third scenario had connectivity equal and increasing as in scenario A,
 162 but u had twice the internal growth rate as v ($r_{uu} = 1.00, r_{vv} = 0.50$, scenario C). Similarly, in scenario D,
 163 u had twice the internal growth rate as v , but r_{vu} increasing from 0.01 to 1.00. Different internal growth rates
 164 could represent different host population sizes or environmental conditions affecting growth on the two farms.

165 In each scenario, for each value of the appropriate control parameters (i.e., r_{vu} , and r_{uv} in scenarios A &
 166 C; Table 1), we simulated the return map over 2000 iterations starting at $u_0^* = 2.7$. We constructed a bifurcation
 167 diagram by plotting the values of $\phi(u^*)$ for the last 500 iterations, over the value of the control parameter. We
 168 present the results for $u_0^* = 2.7$, but we examined the bifurcation diagrams starting from several values of u_0^*
 169 to check that the long-term dynamics were not dependent on the initial conditions (Online Resource, Fig. S1).

170 We also considered the long-term frequency of treatments over increasing connectivity between popula-
 171 tions. To calculate the frequency of treatments, we first iterated the return map 500 times starting at $u^* = 2.7$
 172 to remove transient dynamics and then simulated the dynamical system given by Eq. 2 for 100 treatments,
 173 where treatments were counted across both populations. If the two populations were treated at the same time,
 174 we considered it two treatments. The frequency of treatments was then calculated as 100 divided by the time
 175 taken to reach 100 treatments. To examine how connectivity affects the frequency of treatments independent
 176 of overall increases in the growth rates, we also considered a variation on scenario A in which the internal
 177 growth rate declined as connectivity increased such that $r_{ii} = 1 - r_{ij}$ and the total growth rates to populations
 178 remained constant (Online Resource).

179 2.4 Testing for chaos

180 Under certain parameter values, the numerically-calculated return map given by Eq. (3) had a discontinuity at
 181 the point where u was treated m times or $m + 1$ times, depending on the population density u^* at the first
 182 treatment of v (see Results). This discontinuity resulted in cyclic behaviour that was difficult to classify by
 183 numerical simulations as periodic or chaotic (Galvanetto 2000). Chaos is extreme sensitivity to initial condi-
 184 tions, and can be classified by calculating the rate of divergence between two trajectories that are initially close
 185 (Hastings et al 1993). This rate is known as the Lyapunov exponent λ where $\epsilon_n = \epsilon_0 e^{\lambda n}$, $\epsilon_0 \ll 1$, and ϵ_n
 186 is the difference between a perturbed and fiducial trajectory after n iterations of the return map. Positive expo-
 187 nents indicate that two trajectories will diverge and therefore the dynamics are sensitive to the initial condition,
 188 characteristic of chaos (Sprott 2003; Hastings et al 1993).

189 To determine if the return map lead to chaotic dynamics under the scenarios we considered, we numerically
 190 calculated the Lyapunov exponent for all parameter combinations (Table 1) as,

$$\lambda = \sum_{n=1}^{10^4} \log \left(\frac{|\epsilon_n|}{\epsilon_0} \right). \quad (4)$$

191 For discontinuous return maps such as ours, Eq. (4) is not valid if the fiducial and perturbed trajectories project
 192 onto different pieces of the return map (Galvanetto 2000). To avoid this problem, we chose a small initial
 193 difference between the trajectories of $\epsilon_0 = 10^{-8}$. At each iteration of the return map, we readjusted the two
 194 trajectories bringing them back together along the line of separation such that the difference between them was
 195 ϵ_0 , with the sign of the difference equal to the sign of ϵ_{n-1} (Sprott 2003, p. 116-117):

$$\epsilon_n = \phi \left(\phi^{n-1}(u^*) + \frac{\epsilon_{n-1}}{|\epsilon_{n-1}|} \epsilon_0 \right) - \phi^n(u^*) \quad (5)$$

196 where $\phi^n(u^*)$ represents the n^{th} iteration of the fiducial trajectory (i.e., $\phi^2(u^*) = \phi(\phi(u^*))$). This correction
 197 made it very unlikely that the two trajectories would project onto different pieces of the return map, as the
 198 difference between them remained relatively small. In all our simulations, we verified that $\epsilon_n \ll 1$, suggesting
 199 that the two trajectories had projected on to the pieces of the return map.

200 In the numerical calculation, the value of the Lyapunov exponent may depend on the choice of u_0^* (Earn-
 201 shaw 1993), so we repeated the calculation of Eq. (4) for three randomly-chosen values between N_{\min} and
 202 N_{\max} . For each starting value, we iterated the map 200 times to remove transient dynamics and then used the
 203 subsequent 10 000 iterations in the calculation of λ (Sprott 2003). We report the mean value of λ over the three
 204 values of u_0^* for each value of connectivity described in section 2.3.

205 2.5 Stochasticity

206 Environmental stochasticity may influence the growth of populations, as is the case for sea louse populations on
 207 salmon farms (Aldrin et al 2013; Rogers et al 2013). We added stochasticity to the return map and evaluated its
 208 influence on the long-term dynamics. At each iteration, we multiplied $\phi(u^*)$ by a log-normal distribution with
 209 mean one and standard deviation on the log scale of $s = 10^{-2}$ (Hilborn and Mangel 1997). We compared the
 210 stochastic dynamics for parameters that corresponded to a quasiperiodic cycle with a Lyapunov exponent close
 211 to zero in the deterministic model versus those that produced periodic dynamics or had a single equilibrium
 212 with a Lyapunov exponent that was relatively large and negative in the deterministic model. We examined

213 200 iterations of the return map for two trajectories: one fiducial trajectory starting at $u_0^* = 2.7$ and a second
214 perturbed trajectory initially separated by a small distance $\epsilon_0 = 10^{-8}$ from the fiducial trajectory. We compared
215 the difference between these trajectories over increasing iterations and also calculated the Lyapunov exponent,
216 with and without stochasticity in the model. In calculating the Lyapunov exponent for the stochastic return
217 map, we used an independent sequence of log-normal values for the fiducial and perturbed trajectories. To
218 ensure the value of λ in the stochastic model was not sensitive to the particular log-normal random values in
219 the simulation, we repeated the calculation 50 times and report the mean and range.

220 3 Results

221 3.1 Simulations of simple model

222 Simulations of the model predicted that for two isolated populations (i.e., $r_{ij} = 0 \forall i \neq j$), each population will
223 oscillate with treatments occurring at regular intervals. The frequency of treatments was dictated by the internal
224 population growth rate r_{ii} , with higher growth rates resulting in more rapid resurgence of the population after
225 treatment and therefore a higher frequency of treatments.

226 When we coupled the two populations, the dynamics were more complex. Simulations displayed a range
227 of behaviour including alternating treatments (i.e., phase locking; Fig. 1a), synchrony between the populations
228 (Fig. 1b), or seemingly chaotic dynamics (Fig. 1c; Table 2). To better understand this complex behaviour, we
229 considered a one-dimensional discrete-time return map describing the change in u in between treatments of v .

230 3.2 Discrete-time treatment dynamics

231 For two populations that have identical growth rates but low connectivity, the return map had a stable equi-
232 librium in the open interval (N_{\min}, N_{\max}) (the exact value depended on the level of connectivity) and unstable
233 equilibria at N_{\min} and at N_{\max} . This dynamical behaviour is termed phase locking because the two populations
234 had the same period but their dynamics were shifted out of phase by a fixed amount (Becks and Arndt 2013).
235 The consequence was alternating treatments of u and v , with a stable equilibrium for the population density

236 u whenever v was treated (Fig. 1a & 2a). If both populations were treated at the same time, u was exactly at
 237 the unstable equilibrium. In this case, the two populations remained synchronized because the period of their
 238 oscillations was identical.

239 If the stable equilibrium was at the treatment threshold N_{\min} or N_{\max} , then the dynamics of the two popu-
 240 lations tended towards synchrony. From our limited investigation of parameter space, this was observed when
 241 connectivity between the populations was equal and greater than the internal growth rates of the populations
 242 (i.e., $r_{ij} = r_{ji} > r_{ii} = r_{jj}$; Table 2). Synchrony also occurred if the internal growth rates were unequal, but
 243 the total growth rates of the two populations were equal (i.e., $r_{uu} + r_{uv} = r_{vv} + r_{vu}$) and one population had
 244 a lower growth rate and higher connectivity to the other population. In this case, the population with higher
 245 connectivity became entrained by the dynamics of the “source” population.

246 A third type of behaviour occurred when the total growth rates of the populations were not equal. In this
 247 case, the two populations oscillated with different periods. There was a discontinuity in the return map where
 248 u went from being treated once to twice (or two to three times, depending on the relative growth rates) before
 249 v was treated (Fig. 2c). This discontinuity resulted in periodic or seemingly chaotic behaviour. Unlike in phase
 250 locking or synchrony, the population density u was not the same each time v was treated (Fig. 1c).

Table 2 Summary of parameter values under which different dynamics were observed.

Internal growth rate	Connectivity	Behaviour	Figure
$r_{uu} = r_{vv}$	$(r_{uv} = r_{vu}) \leq (r_{uu} = r_{vv})$	Phase locking	Fig. 2a
	$(r_{uv} = r_{vu}) > (r_{uu} = r_{vv})$	Synchrony	Fig. 2b & 4a
	$r_{uv} \neq r_{vu}$	Cycles	
$r_{uu} \neq r_{vv}$	$r_{uv} = r_{vu}$; incl. $r_{uv} = r_{vu} = 0$	Cycles	Fig. 2c
	$(r_{uu} + r_{uv}) = (r_{vu} + r_{vv})$	Synchrony or phase locking	Fig. 4b & S8
	Else	Phase locking or cycles	Fig. 2c

251 3.3 Parameter sensitivity

252 Increasing the connectivity between two patches resulted in changes to the long-term values of $\phi(u^*)$, the
 253 population density at re-treatment (Fig. 3 and Fig. S1). Some of these changes happened abruptly when the

254 connectivity crossed a threshold (Fig. 3c,d) while others happened gradually (Fig. 3a). When the two popu-
 255 lations had equal internal growth rates and equal connectivity, increasing the connectivity lead to increasing
 256 population density at re-treatment, until connectivity equalled the internal growth rates (scenario A in Table 1;
 257 Fig. 3a). At that point, the dynamics were phase-locked such that the population density at re-treatment was
 258 always the initial population density (i.e., $(\phi(u^*) = u^*) \forall u^*$; see Online Resource Figs S2-S5 for illustrative
 259 animations).

260 When connectivity was increased from u to v only (e.g., scenario B in Table 1), the return map had a
 261 discontinuity because the total growth rate of v was higher than that of u . In that case, we observed periodic
 262 dynamics, the simplest being a two-point cycle that occurred near $r_{vu} = 0.8$ (Fig. 3b). In these two point
 263 cycles, after the initial treatment of v , u will be treated once, then after the next treatment of v , u will be treated
 264 twice. This cycle repeats itself resulting in a pattern of treatments $v, u, v, u, u, v, u, v, u, u, u$, etc., with u having
 265 a lower population density at the treatment of v if u has been treated twice since the previous treatment of v .

266 When the internal growth rates of the populations were not equal (i.e., scenarios C and D in Table 1),
 267 the dynamics tended to be cyclic (Fig. 3c,d). However, abrupt changes from cyclic dynamics to stable points
 268 occurred as connectivity was increased to the point where the return map touched or crossed the 1:1 line.
 269 For example, in scenario D, when r_{vu} neared 0.51, the dynamics tended towards phase locking (Fig. S5). As
 270 connectivity increased from $r_{vu} = 0.35$ to $r_{vu} = 0.51$, the stable point approached N_{\min} and the magnitude of
 271 the rescue effect decreased because u had a lower population density on treatment of v . When the total growth
 272 rates were exactly equal (i.e., $r_{vu} = 0.51$ such that $(r_{uu} + r_{uv}) = (r_{vu} + r_{vv})$), the two populations became
 273 synchronized (Fig. 3d; Table 2).

274 Increasing the connectivity between the patches did not necessarily result in a monotonic increase in the
 275 frequency of treatments (Fig. S6). For illustration, we focus on the frequency of treatments under scenario A,
 276 but with connectivity increasing to $r_{uv} = r_{vu} = 2.00$, and on scenario D with connectivity between $r_{vu} =$
 277 0.35 and 0.52. In these scenarios, the internal growth rates were held constant (Table 1). Thus, we expected that
 278 the frequency of treatments would increase with increasing connectivity because the the total growth rate to the
 279 populations was increasing. However, we observed a sharp decline in the frequency of treatments in scenario

280 A when connectivity exceeded the internal growth rate (Fig. 4a). In scenario D, the frequency of treatments
281 declined over the region of phase locking (see Fig. 3d) as the stable point approached N_{\min} , reducing the impact
282 of the rescue-effect. The minimum frequency of treatments occurred where populations became synchronized
283 at $r_{vu} + r_{vv} = r_{uv} + r_{uu}$ (i.e., $r_{vu} = 0.51$, Fig. 4b). In the Online Resrouce, we also considered a decline in the
284 internal growth rate as connectivity increased such that $r_{ii} = 1 - r_{ij}$ and the total growth rates to populations
285 remained constant in order to examine how connectivity affects the frequency of treatments independent of
286 overall increases in the growth rates. These simulations also showed a decrease in the frequency of treatments
287 when populations became synchronized, and frequency of treatments remained low as connectivity increased
288 further (Fig. S7).

289 3.4 Testing for chaos

290 The time series of population density appeared chaotic when the period of the population cycles in the two
291 patches was different (Fig. 1c). The bifurcation diagrams showed large regions of parameter space that had
292 potentially chaotic dynamics (Fig. 1c and Fig. 3c-d). However, the Lyapunov exponent was not greater than
293 zero in any of the scenarios (Fig. 3c-d), indicating the dynamics were not chaotic. Instead, the dynamics of two
294 populations with different internal periods of oscillations appeared quasiperiodic. For periodic cycles, after
295 iterating the return map a finite number of times, we returned to the exact value at which we started (e.g., Fig.
296 5b). Quasiperiodic cycles are differentiated from periodic cycles by cobwebbing the return map; over several
297 treatments of v , $\phi(u^*)$ returned to the original branch of the return map very near to the starting point but
298 not exactly at the starting point, such that the dynamics were shifted slightly (e.g., Fig. 5d). We note that a
299 precise distinction between quasiperiodic and periodic dynamics is limited by the the number of times we
300 could numerically iterate the return map.

301 3.5 Stochasticity

302 Small amounts of stochasticity added to the return map tended to shift quasiperiodic dynamics towards chaos
303 such that two population initially close had very different population densities after 200 iterations. However,
304 when the dynamics were periodic, the stochasticity was damped such that the fiducial trajectory and the per-
305 turbed trajectory remained relatively close over 200 iterations of the return map (Fig. 5a). A small change in
306 r_{vu} from 0.72 to 0.71 in scenario C caused a transition from periodic to quasiperiodic dynamics (Fig. 5b,d).
307 In the quasiperiodic case, the two trajectories drifted apart as the stochasticity accumulated (Fig. 5c). For
308 scenario D, when r_{vu} was increased from 0.31 to 0.32, the deterministic dynamics went from quasiperiodic
309 to phase locking (Fig. 3d). In this case, as in scenario C, stochasticity caused the trajectories to diverge for
310 $r_{vu} = 0.31$ corresponding to the quasiperiodic dynamics, but stochasticity was damped when the deterministic
311 dynamics exhibited phase locking (Fig. S9). This shows that small amounts of stochasticity can accumulate,
312 when dynamics are not stable or periodic, and result in sensitivity to initial conditions that is characteristic
313 of chaotic dynamics. Indeed, the Lyapunov exponents for the stochastic version of the model shown in Fig. 5
314 were $\lambda = 14.19$ (range 14.16 to 14.21) for $r_{vu} = 0.71$, compared to $\lambda = -0.001$ for the deterministic model.
315 The Lyapunov exponent was also positive but smaller for the periodic dynamics corresponding to $r_{vu} = 0.72$,
316 which showed damped oscillations (Fig. 5a).

317 4 Discussion

318 The current magnitude and extent of coupled human and natural systems is unprecedented and there is an
319 urgent need to better understand the consequences of accelerating human impacts on natural ecosystems and
320 the services that they provide (Millennium Ecosystem Assessment 2005). In this study, we considered the
321 reciprocal interactions between the natural dynamics of parasite populations and human intervention in the
322 form of parasite control. The resulting dynamics were surprisingly complex, and demonstrate the potential for
323 unexpected behaviour to result in policies that are well-meaning but have unintended and potentially perverse
324 consequences for the health of ecosystems.

325 4.1 Implications for sea louse management

326 In Pacific Canada, salmon farms must treat with chemotherapeutants when sea louse populations exceed three
327 motile sea lice per fish, a guideline that is meant to protect juvenile wild salmon from sea louse infestations
328 during a vulnerable period of their migration (British Columbia Ministry of Agriculture and Lands 2005;
329 Brooks 2009). However, our model showed that strict threshold control of parasites according to this policy
330 may lead to asynchronous or even chaotic dynamics on adjacent farms connected by dispersal. In practice,
331 whether dynamics are truly chaotic may not matter; given the timeframe of observations and management de-
332 cisions, periodic dynamics may be just as challenging to predict and control. Increasing connectivity between
333 populations tended to increase the frequency of treatments, unless populations were synchronized. Frequent,
334 uncoordinated treatments are a problem because they may hasten the evolution of sea louse resistance to current
335 chemotherapeutants by allowing sea lice that are resistant to treatment to disperse and find mates on nearby,
336 untreated farms (Aaen et al 2015). Further, asynchronous parasite dynamics among farms make it difficult
337 to ensure low parasite abundance during the wild juvenile salmon migration. Paradoxically, because thresh-
338 old treatments tend to decouple parasite populations when not coordinated, this well-intended policy could
339 mean high sea louse abundances on salmon farms along the migration route, transmission to juvenile salmon
340 (Krkošek et al 2006; Marty et al 2010) and adverse impacts on wild salmon populations (Krkošek et al 2011;
341 Peacock et al 2013).

342 The current treatment threshold policy does reduce louse abundance on farms, but more coordinated efforts
343 to synchronize the parasite dynamics among farms may reduce reliance on chemotherapeutants. We found that
344 at low levels of dispersal, the frequency of treatments increased with increasing connectivity, suggesting that
345 dispersal among farms hinders control efforts. However, the frequency of treatments declined substantially
346 when connectivity was high enough that parasite dynamics were synchronized between farms (Fig. 4a). In re-
347 ality, dispersal of sea lice among farms is likely too low to synchronize parasite dynamics on adjacent farms by
348 itself (Adams et al 2012; Foreman et al 2015, although shared environmental effects may help, see below). But
349 for populations that were weakly coupled but had similar internal growth rates (e.g., have a similar number/age

350 of hosts and are exposed to similar environmental conditions), synchrony could be induced by either treating
351 populations at the same time (even if one population had not reached the threshold) or coordinating stocking
352 and harvest among adjacent farms so that they start with the same initial conditions. Such strategies may reduce
353 the potential for the rescue effect in louse populations on adjacent farms and therefore lower the frequency of
354 treatments, but require coordinated effort among multiple stakeholders (e.g., different levels of government and
355 industry). Pest management plans that require this kind of cooperation have been recommended (e.g., Brooks
356 2009; Peacock et al 2013), but are still not implemented in many areas, including Pacific Canada.

357 4.2 Model limitations

358 Our simple model did not consider exogenous forces on the population dynamics such as variability in growth
359 rates due to shared environmental conditions. Such forces are likely, due to the effect of temperature and
360 salinity on settlement success (Bricknell et al 2006), developmental rates (Groner et al 2014; Stien et al 2005)
361 and survival (Johnson and Albright 1991a) of sea lice. Environmental conditions have been proposed to result
362 in synchrony of local population dynamics over wide geographic scales (i.e., Moran effects; Moran 1953).
363 Indeed, such an effect has been shown in a variety of systems (e.g., Cheal et al 2007; Grenfell et al 1998).
364 Sea louse populations on farmed salmon show annual cycles (Marty et al 2010) that may be driven, in part, by
365 changes in salinity and/or temperature (Johnson and Albright 1991b). The relative contributions of dispersal
366 versus environment in driving synchrony of local populations is an ongoing question in ecology (Lande et al
367 1999), and sea lice in networks of salmon farms may provide an ideal model system due to the extensive
368 monitoring of louse populations and environmental conditions on salmon farms. These data have been used in
369 statistical analyses aimed at management applications (e.g., Rogers et al 2013; Revie et al 2003), but could also
370 be useful in answering questions of general interest in ecology.

371 4.3 Dynamics of coupled populations

372 There has been considerable theoretical interest in how dispersal affects the dynamics of coupled populations
373 (e.g., Dey et al 2014, 2015; Hastings et al 1993; Kendall and Fox 1998; Goldwyn and Hastings 2011; Franco
374 and Ruis-Herrera 2015). Our analysis expands on previous theoretical work in several ways. First, we consid-
375 ered control of populations when a threshold abundance was reached. Previous work has considered density
376 dependence as part of the intrinsic dynamics of local populations (e.g., the Ricker model, Dey et al 2015;
377 Hastings et al 1993) or periodic interventions such as feeding and harvest (e.g., Chau 2000). We consider a
378 nonlinear reciprocal interaction between parasite populations and control intervention that had not yet been
379 explored, although our approach shares similarities with work on Adaptive Limiter Control, discussed below
380 (e.g., Sah et al 2013). Second, we analyzed a continuous-time population model that may be more represen-
381 tative for some species, but were able to simplify our analysis by considering a discrete time return map for
382 the population density in one patch at the time of treatment in the other. This dynamical-systems approach has
383 gained attention recently in the context of peak to peak dynamics (Rinaldi et al 2001) and statistical methods
384 for analyzing time series data (Sugihara et al 2012), but also has broader applications for simplifying analyses
385 of continuous-time models for interacting populations (Schaffer 1985). Finally, we varied both the internal
386 growth rates and connectivities in our populations to explore scenarios where growth rates of the two pop-
387 ulations differed and connectivity was not necessarily reciprocal. Many studies of coupled populations only
388 consider equal connectivity (although see Dey et al 2014; Franco and Ruis-Herrera 2015).

389 Increasing connectivity between two populations subject to control was expected to increase the frequency
390 of treatments, but the simple model we developed displayed much more complex dynamics. Our results were
391 consistent with other population models that show high connectivity leads to synchrony of populations while
392 lower levels of connectivity lead to out-of-phase dynamics (Dey et al 2015, 2014). If the two populations had
393 different periods due to unequal growth rates, the dynamics underwent periodic or quasiperiodic cycles. When
394 dynamics were periodic, added stochasticity was damped such that the difference between nearby trajectories
395 remained small. Hastings (Hastings 1993) analyzed a coupled discrete logistic model and also found that the

396 addition of stochasticity resulted in chaos for parameter values corresponding to a four-point cycle in the
397 deterministic model, but stable population densities for parameter values corresponding to a two-point cycle
398 in the deterministic model. This result highlights the fine line between predictable deterministic dynamics and
399 chaos (Hastings 1993).

400 Previous work on threshold interventions in population dynamics have incorporated Adaptive Limiter Con-
401 trol (ALC; e.g., Sah et al 2013). ALC involves a threshold intervention as in our model, but works to the oppo-
402 site effect: where we consider control of a population when it goes above a threshold, ALC avoids population
403 crashes by forcing immigration when the population drops below a threshold. Despite this difference, high
404 thresholds for ALC tend to decouple subpopulations in a similar manner to our strict treatment threshold (Sah
405 et al 2013). This decoupling has opposite effects on fluctuations of the metapopulation depending on the migra-
406 tion rate between subpopulations. At high migration rates, subpopulations tend to be positively correlated, such
407 that decoupling due to ALC is effective at increasing stability of the overall metapopulation. However, at low
408 migration rates, subpopulations are more likely to be fluctuating out of phase and therefore ALC exacerbates
409 this negative synchrony and decreases metapopulation stability. Sah et al (2013) found both theoretical and
410 empirical evidence that these effects of ALC generally act to increase persistence of populations and metapop-
411 ulations. Considering populations of pests and pathogens, persistence is not the desired outcome, providing an
412 intriguing possibility that by decoupling populations, threshold effects may actually hinder eradication unless
413 coordinated.

414 4.4 Conclusion

415 The complexity of coupled human and natural systems has gained attention as we recognize and attempt to
416 understand our impact on natural ecosystems. For aquaculture, the interaction between farm management and
417 natural pathogen dynamics, including dispersal among farms, may lead to unpredictable dynamics that under-
418 mine our ability to maintain a healthy environment for both farmed and wild salmon. The successful manage-
419 ment of disease in coastal ecosystems likely requires cooperation among different companies to synchronize

420 and stabilize pathogen dynamics. This example emphasizes that human-natural couplings cross the boundaries
421 of policy and governance, and cooperation among stakeholders at different levels is required to achieve the
422 common goal of healthy and sustainable ecosystems that can support adaptive human populations.

423 **Acknowledgements** We thank three reviewers and the Handling Editor for constructive feedback on earlier versions. Funding
424 for this work came from the Natural Sciences and Engineering Research Council of Canada (Vanier CGS to SJP, PDF to AWB,
425 Discovery and Accelerator grants to MAL and MK), a Bill Shostak Wildlife Award and Fisher Scientific Scholarship to SJP, a
426 Canada Research Chair and Killam Fellowship to MAL, a Sloan Fellowship in Ocean Science to MK, and a Killam Postdoctoral
427 Fellowship to AWB. No funders had input into the design of the study.

428 References

- 429 Aaen SM, Helgesen KO, Bakke MJ, Kaur K, Horsberg TE (2015) Drug resistance in sea lice: a threat to
430 salmonid aquaculture. *Trends in Parasitology* 31(2):72–81, doi: 10.1016/j.pt.2014.12.006, URL [http://](http://linkinghub.elsevier.com/retrieve/pii/S1471492214002098)
431 linkinghub.elsevier.com/retrieve/pii/S1471492214002098
- 432 Abbott KC (2011) A dispersal-induced paradox: Synchrony and stability in stochastic metapopulations. *Ecology Letters* 14(11):1158–1169, doi: 10.1111/j.1461-0248.2011.01670.x
- 433 Adams T, Black K, Macintyre C, Macintyre I, Dean R (2012) Connectivity modelling and network analysis
434 of sea lice infection in Loch Fyne, west coast of Scotland. *Aquaculture Environment Interactions* 3:51–63,
435 doi: 10.3354/aei00052, URL <http://www.int-res.com/abstracts/aei/v3/n1/p51-63/>
- 436 Aldrin M, Storvik B, Kristoffersen AB, Jansen PA (2013) Space-Time Modelling of the Spread of Salmon Lice
437 between and within Norwegian Marine Salmon Farms. *PLoS ONE* 8(5):e64,039, doi: 10.1371/journal.pone.
438 0064039, URL <http://dx.doi.org/10.1371/journal.pone.0064039>
- 439 Becks L, Arndt H (2013) Different types of synchrony in chaotic and cyclic communities. *Nature com-*
440 *munications* 4:1359, doi: 10.1038/ncomms2355, URL [http://www.ncbi.nlm.nih.gov/pubmed/](http://www.ncbi.nlm.nih.gov/pubmed/23322047)
441 [23322047](http://www.ncbi.nlm.nih.gov/pubmed/23322047)
- 442 Birch L (1948) The intrinsic rate of natural increase of an insect population. *The Journal of Animal Ecology*
443 pp 15–26, URL www.jstor.org/stable/1605
- 444 Bolker BM, Grenfell BT (1996) Impact of vaccination on the spatial correlation and persistence of measles
445 dynamics. *Proceedings of the National Academy of Sciences* 93(22):12,648–12,653, URL [http://www.](http://www.pnas.org/content/93/22/12648.abstract)
446 [pnas.org/content/93/22/12648.abstract](http://www.pnas.org/content/93/22/12648.abstract)
- 447 Bricknell IR, Dalesman SJ, O’Shea B, Pert CC, Luntz AJM (2006) Effect of environmental salinity on sea lice
448 *Lepeophtheirus salmonis* settlement success. *Diseases of Aquatic Organisms* 71(3):201–212, doi: 10.3354/
449 [dao071201](http://www.int-res.com/abstracts/dao/v71/n3/p201-212/), URL <http://www.int-res.com/abstracts/dao/v71/n3/p201-212/>
- 450 British Columbia Ministry of Agriculture and Lands (2005) Fish Health Program 2003-2005. Tech. rep.,
451 Ministry of Agriculture and Lands, URL [http://www.agf.gov.bc.ca/ahc/fish{ }](http://www.agf.gov.bc.ca/ahc/fish{ }health/)
452 [Fish{ }Health{ }Report{ }2003-2005.pdf](http://www.agf.gov.bc.ca/ahc/fish{ }health/)
- 453 Brooks EN, Lebreton JD (2001) Optimizing removals to control a metapopulation: Application to the
454 yellow legged herring gull (*Larus cachinnans*). *Ecological Modelling* 136(2-3):269–284, doi: 10.1016/
455 [S0304-3800\(00\)00430-0](http://www.elsevier.com/locate/ecolmodel)
- 456 Brooks KM (2009) Considerations in developing an integrated pest management programme for
457 control of sea lice on farmed salmon in Pacific Canada. *Journal of Fish Diseases* 32(1):59–73,
458 URL [http://login.ezproxy.library.ualberta.ca/login?url=http://search.](http://login.ezproxy.library.ualberta.ca/login?url=http://search.ebscohost.com/login.aspx?direct=true{%&db=ehi{%&AN=36551408{%&site=ehost-live{%&scope=site)
459 [ebscohost.com/login.aspx?direct=true{%&db=ehi{%&AN=36551408{%&site=](http://login.ezproxy.library.ualberta.ca/login?url=http://search.ebscohost.com/login.aspx?direct=true{%&db=ehi{%&AN=36551408{%&site=ehost-live{%&scope=site)
460 [ehost-live{%&scope=site](http://login.ezproxy.library.ualberta.ca/login?url=http://search.ebscohost.com/login.aspx?direct=true{%&db=ehi{%&AN=36551408{%&site=ehost-live{%&scope=site)

- 462 Brown JHJ, Kodric-Brown A (1977) Turnover rates in insular biogeography: effect of immigration on extinc-
463 tion. *Ecology* 58(2):445–449, doi: 10.2307/1935620, URL [http://www.esajournals.org/doi/](http://www.esajournals.org/doi/abs/10.2307/1935620)
464 [abs/10.2307/1935620](http://www.esajournals.org/doi/abs/10.2307/1935620)
- 465 Chau NP (2000) Destabilising effect of periodic harvest on population dynamics. *Ecological Mod-*
466 *elling* 127(1):1–9, doi: 10.1016/S0304-3800(99)00190-8, URL [http://www.sciencedirect.com/](http://www.sciencedirect.com/science/article/pii/S0304380099001908)
467 [science/article/pii/S0304380099001908](http://www.sciencedirect.com/science/article/pii/S0304380099001908)
- 468 Cheal AJ, Delean S, Sweatman H, Thompson AA (2007) Spatial synchrony in coral reef fish populations and
469 the influence of climate. *Ecology* 88(1):158–69, doi: 10.1890/0012-9658(2007)88[158:SSICRF]2.0.CO;2,
470 URL <http://www.ncbi.nlm.nih.gov/pubmed/17489464>
- 471 Costello MJ (2009) How sea lice from salmon farms may cause wild salmonid declines in Eu-
472 rope and North America and be a threat to fishes elsewhere. *Proceedings of the Royal Society*
473 *B: Biological Sciences* 276(1672):3385–3394, doi: 10.1098/rspb.2009.0771, URL [http://rspb.](http://rspb.royalsocietypublishing.org/content/276/1672/3385)
474 [royalsocietypublishing.org/content/276/1672/3385](http://rspb.royalsocietypublishing.org/content/276/1672/3385)
- 475 Dey S, Goswami B, Joshi A (2014) Effects of symmetric and asymmetric dispersal on the dynamics of het-
476 erogeneous metapopulations: Two-patch systems revisited. *Journal of Theoretical Biology* 345:52–60, doi:
477 10.1016/j.jtbi.2013.12.005, URL <http://dx.doi.org/10.1016/j.jtbi.2013.12.005>
- 478 Dey S, Goswami B, Joshi A (2015) A possible mechanism for the attainment of out-of-phase periodic dynamics
479 in two chaotic subpopulations coupled at low dispersal rate. *Journal of Theoretical Biology* 367:100–110,
480 doi: 10.1016/j.jtbi.2014.11.028, URL <http://dx.doi.org/10.1016/j.jtbi.2014.11.028>
- 481 Earn DJD, Rohani P, Grenfell BT (1998) Persistence, chaos and synchrony in ecology and epidemiology.
482 *Proceedings of the Royal Society of London Series B: Biological Sciences* 265(1390):7–10, URL [http:](http://rspb.royalsocietypublishing.org/content/265/1390/7.abstract)
483 [//rspb.royalsocietypublishing.org/content/265/1390/7.abstract](http://rspb.royalsocietypublishing.org/content/265/1390/7.abstract)
- 484 Earnshaw JC (1993) Lyapunov exponents for pedestrians. *American Journal of Physics* 61(5):401, doi: 10.
485 1119/1.17231, URL [http://scitation.aip.org/content/aapt/journal/ajp/61/5/10.](http://scitation.aip.org/content/aapt/journal/ajp/61/5/10.1119/1.17231)
486 [1119/1.17231](http://scitation.aip.org/content/aapt/journal/ajp/61/5/10.1119/1.17231)
- 487 FAO (2014) The State of World Fisheries and Aquaculture 2014. Tech. rep., Food and Agriculture Organization
488 of the United Nations, Rome, URL www.fao.org/publications
- 489 Foreman MGG, Chandler PC, Stucchi DJ, Garver KA, Guo M, Morrison J, Tuele D (2015) The ability of
490 hydrodynamic models to inform decisions on the siting and management of aquaculture facilities in British
491 Columbia. *Canadian Science Advisory Secretariat Research Document* 2015/005:vii + 49 p., URL [http:](http://www.dfo-mpo.gc.ca/csas-sccs/)
492 [//www.dfo-mpo.gc.ca/csas-sccs/](http://www.dfo-mpo.gc.ca/csas-sccs/)
- 493 Franco D, Ruis-Herrera A (2015) To connect or not to connect isolated patches. *Journal of Theoretical Biology*
494 370:72–80, doi: 10.1016/j.jtbi.2015.01.029, URL [http://dx.doi.org/10.1016/j.jtbi.2015.](http://dx.doi.org/10.1016/j.jtbi.2015.01.029)
495 [01.029](http://dx.doi.org/10.1016/j.jtbi.2015.01.029)
- 496 Frazer LN, Morton A, Krkošek M (2012) Critical thresholds in sea lice epidemics: evidence, sensitivity and
497 subcritical estimation. *Proceedings of the Royal Society B: Biological Sciences* 279(1735):1950–1958, doi:
498 10.1098/rspb.2011.2210, URL [http://rspb.royalsocietypublishing.org/content/279/](http://rspb.royalsocietypublishing.org/content/279/1735/1950)
499 [1735/1950](http://rspb.royalsocietypublishing.org/content/279/1735/1950)
- 500 Fulford G, Roberts M, Heesterbeek J (2002) The Metapopulation Dynamics of an Infectious Disease: Tu-
501 berculosis in Possums. *Theoretical Population Biology* 61(1):15–29, doi: 10.1006/tpbi.2001.1553, URL
502 <http://linkinghub.elsevier.com/retrieve/pii/S0040580901915539>
- 503 Galvanetto U (2000) Numerical computation of Lyapunov exponents in discontinuous maps implicitly de-
504 fined. *Computer Physics Communications* 131(1):1–9, doi: 10.1016/S0010-4655(00)00055-2, URL [http:](http://www.sciencedirect.com/science/article/pii/S0010465500000552)
505 [//www.sciencedirect.com/science/article/pii/S0010465500000552](http://www.sciencedirect.com/science/article/pii/S0010465500000552)
- 506 Goldwyn EE, Hastings A (2011) The roles of the Moran effect and dispersal in synchronizing oscillating
507 populations. *Journal of Theoretical Biology* 289(1):237–246, doi: 10.1016/j.jtbi.2011.08.033, URL [http:](http://dx.doi.org/10.1016/j.jtbi.2011.08.033)
508 [//dx.doi.org/10.1016/j.jtbi.2011.08.033](http://dx.doi.org/10.1016/j.jtbi.2011.08.033)
- 509 Grenfell BT, Wilson K, Finkenstadt BF, Coulson TN, Murray S, Albon SD, Pemberton JM, Clutton-Brock TH,
510 Crawley MJ (1998) Noise and determinism in synchronized sheep dynamics. *Nature* 394(6694):674–677,
511 doi: 10.1038/29291, URL <http://dx.doi.org/10.1038/29291>

- 512 Groner ML, Gettinby G, Stormoen M, Revie CW, Cox R (2014) Modelling the impact of temperature-induced
513 life history plasticity and mate limitation on the epidemic potential of a marine ectoparasite. PLoS ONE
514 9(2):e88465, URL <http://dx.doi.org/10.1371/journal.pone.0088465>
- 515 Hastings A (1993) Complex interactions between dispersal and dynamics: lessons from coupled logistic equa-
516 tions. Ecology 74(5):1362–1372, doi: 10.2307/1940066
- 517 Hastings A, Powell T (1991) Chaos in a three species food chain. Ecology 72(3):896–903, URL [http://](http://www.jstor.org/stable/1940591)
518 www.jstor.org/stable/1940591
- 519 Hastings A, Hom CL, Ellner S, Turchin P, Godfray HCJ (1993) Chaos in Ecology: Is Mother Nature a Strange
520 Attractor? Annual Review of Ecology and Systematics 24(1):1–33, doi: 10.1146/annurev.es.24.110193.
521 000245, URL <http://www.jstor.org/discover/10.2307/2097171>
- 522 Heggberget TG, Johnsen BO, Hindar K, Jonsson B, Hansen LP, Hvidsten Na, Jensen AJ (1993) Interactions
523 between wild and cultured Atlantic salmon: a review of the Norwegian experience. Fisheries Research 18(1-
524 2):123–146, doi: 10.1016/0165-7836(93)90044-8
- 525 Hilborn R, Mangel M (1997) The Ecological Detective: Confronting Models with Data, Monographs in Popu-
526 lation Biology, vol 28. Princeton University Press
- 527 Holt RD, McPeck MA (1996) Chaotic population dynamics favors the evolution of dispersal. American Natu-
528 ralist 148(4):709–718, doi: 10.2307/2678832, URL <http://www.jstor.org/stable/2556325>
- 529 Igboeli OO, Burka JF, Fast MD (2014) *Lepeophtheirus salmonis*: a persisting challenge for salmon aquaculture.
530 Animal Frontiers 4(1):22–32, doi: 10.2527/af.2014-0004, URL [https://dl.sciencesocieties.](https://dl.sciencesocieties.org/publications/af/abstracts/4/1/22)
531 [org/publications/af/abstracts/4/1/22](https://dl.sciencesocieties.org/publications/af/abstracts/4/1/22)
- 532 Ives AR, Settle WH (1997) Metapopulation Dynamics and Pest Control in Agricultural Systems. American
533 Naturalist 149(2):220–246
- 534 Jansen PA, Kristoffersen AB, Viljugrein H, Jimenez D, Aldrin M, Stien A (2012) Sea lice as
535 a density-dependent constraint to salmonid farming. Proceedings of the Royal Society B: Bi-
536 ological Sciences 279(1737):2330–2338, doi: 10.1098/rspb.2012.0084, URL [http://rspb.](http://rspb.royalsocietypublishing.org/content/279/1737/2330.abstract)
537 [royalsocietypublishing.org/content/279/1737/2330.abstract](http://rspb.royalsocietypublishing.org/content/279/1737/2330.abstract)
- 538 Johnson SC, Albright LJ (1991a) Development, Growth, and Survival of *Lepeophtheirus salmonis* (Cope-
539 poda: Caligidae) Under Laboratory Conditions. Journal of the Marine Biological Association of the United
540 Kingdom 71(02):425–436, doi: 10.1017/S0025315400051687, URL [http://dx.doi.org/10.1017/](http://dx.doi.org/10.1017/S0025315400051687)
541 [S0025315400051687](http://dx.doi.org/10.1017/S0025315400051687)
- 542 Johnson SC, Albright LJ (1991b) The developmental stages of *Lepeophtheirus salmonis* (Krøyer, 1837) (Cope-
543 poda: Caligidae). Canadian Journal of Zoology 69(4):929–950, URL [http://dx.doi.org/10.1017/](http://dx.doi.org/10.1017/S0025315400051687)
544 [S0025315400051687](http://dx.doi.org/10.1017/S0025315400051687)
- 545 Keeling MJ, Gilligan Ca (2000) Metapopulation dynamics of bubonic plague. Nature 407(6806):903–906,
546 doi: 10.1038/35038073
- 547 Kendall BE, Fox GA (1998) Spatial structure, environmental heterogeneity, and population dynamics: analysis
548 of the coupled logistic map. Theoretical population biology 54(1):11–37, doi: 10.1006/tpbi.1998.1365
- 549 Kristoffersen AB, Rees EE, Stryhn H, Ibarra R, Campisto JL, Revie CW, St-Hilaire S (2013) Understanding
550 sources of sea lice for salmon farms in Chile. Preventive Veterinary Medicine 111(1-2):165–75, doi: 10.
551 1016/j.prevetmed.2013.03.015, URL <http://www.ncbi.nlm.nih.gov/pubmed/23628338>
- 552 Krkošek M, Lewis MA, Morton A, Frazer LN, Volpe JP (2006) Epizootics of wild fish induced by
553 farm fish. Proceedings of the National Academy of Sciences 103(42):15,506–15,510, doi: 10.1073/pnas.
554 0603525103, URL [http://www.pubmedcentral.nih.gov/articlerender.fcgi?artid=](http://www.pubmedcentral.nih.gov/articlerender.fcgi?artid=1591297&tool=pmcentrez&rendertype=abstract)
555 [1591297&tool=pmcentrez&rendertype=abstract](http://www.pubmedcentral.nih.gov/articlerender.fcgi?artid=1591297&tool=pmcentrez&rendertype=abstract)
- 556 Krkošek M, Bateman A, Proboyszcz S, Orr C (2010) Dynamics of outbreak and control of salmon lice on
557 two salmon farms in the Broughton Archipelago, British Columbia. Aquaculture Environment Interac-
558 tions 1(2):137–146, doi: 10.3354/aei00014, URL [http://www.int-res.com/abstracts/aei/](http://www.int-res.com/abstracts/aei/v1/n2/p137-146/)
559 [v1/n2/p137-146/](http://www.int-res.com/abstracts/aei/v1/n2/p137-146/)
- 560 Krkošek M, Connors BM, Morton A, Lewis MA, Dill LM, Hilborn R (2011) Effects of parasites from salmon
561 farms on productivity of wild salmon. Proceedings of the National Academy of Sciences 108(35):14,700–
562 14,704, doi: 10.1073/pnas.1101845108, URL <http://www.pnas.org/content/108/35/14700>

- 563 Lande R, Engen Steinar, Sæther B (1999) Spatial Scale of Population Synchrony: Environmental Correlation
564 versus Dispersal and Density Regulation. *The American Naturalist* 154(3):271–281, doi: 10.1086/303240,
565 URL <http://www.jstor.org/stable/10.1086/303240>
- 566 Lees F, Baillie M, Gettinby G, Revie CW (2008) The efficacy of emamectin benzoate against infestations
567 of *Lepeophtheirus salmonis* on farmed Atlantic salmon (*Salmo salar* L) in Scotland, 2002–2006. *PLoS*
568 *ONE* 3(2), URL <http://journals.plos.org/plosone/article?id=10.1371/journal.pone.0001549>
- 570 Levins R (1969) Some Demographic and Genetic Consequences of Environmental Heterogeneity for Bi-
571 ological Control. *Bulletin of the Ecological Society of America* 15(3):237–240, URL <http://besa.oxfordjournals.org/content/15/3/237>
- 573 Liebhold A, Koenig WD, Bjørnstad ON (2004) Spatial synchrony in population dynamics. *Annual Review*
574 *of Ecology and Systematics* 35:467–490, doi: 10.1146/annurev.ecolsys.34.011802.132516, URL <http://www.annualreviews.org/doi/full/10.1146/annurev.ecolsys.34.011802.132516>
- 576 Liu J, Dietz T, Carpenter SR, Alberti M, Folke C, Moran E, Pell AN, Deadman P, Kratz T, Lubchenco J, Ostrom
577 E, Ouyang Z, Provencher W, Redman CL, Schneider SH, Taylor WW (2007) Complexity of coupled human
578 and natural systems. *Science* 317(5844):1513, doi: 10.1126/science.1144004, URL <http://www.ncbi.nlm.nih.gov/pubmed/17872436>
- 580 Marty GD, Saksida SM, Quinn TJ (2010) Relationship of farm salmon, sea lice, and wild salmon populations.
581 *Proceedings of the National Academy of Sciences* 107(52):22,599–22,604, doi: 10.1073/pnas.1009573108,
582 URL <http://www.pnas.org/content/107/52/22599.abstract>
- 583 McCallum H, Harvell D, Dobson A (2003) Rates of spread of marine pathogens. *Ecology Letters* 6:1062–
584 1067, doi: 10.1046/j.1461-0248.2003.00545.x, URL onlinelibrary.wiley.com/doi/10.1046/j.1461-0248.2003.00545.x/pdf
- 586 Millennium Ecosystem Assessment (2005) *Ecosystems and Human Well-being: Synthesis*, vol 5. Is-
587 land Press, Washington, DC, doi: 10.1196/annals.1439.003, URL [http://www.who.int/entity/globalchange/ecosystems/ecosys.pdf\\$\\delimiter"026E30F\\$nhhttp://www.loc.gov/catdir/toc/ecip0512/2005013229.html](http://www.who.int/entity/globalchange/ecosystems/ecosys.pdf$\\delimiter)
- 590 Moran PAP (1953) The statistical analysis of the Canadian Lynx cycle II. Synchronization and meteorol-
591 ogy. *Australian Journal of Zoology* 1:291–298, doi: 10.1071/ZO9530291, URL <http://www.publish.csiro.au/?paper=Z09530291>
- 593 Oerke EC (2006) Crop losses to pests. *The Journal of Agricultural Science* 144(01):31, doi: 10.1017/S0021859605005708
- 595 Peacock SJ, Krkošek M, Probošycz S, Orr C, Lewis MA (2013) Cessation of a salmon decline with con-
596 trol of parasites. *Ecological Applications* 23(3):606–620, doi: 10.1890/12-0519.1, URL <http://www.esajournals.org/doi/abs/10.1890/12-0519.1>
- 598 Rae GH (2002) Sea louse control in Scotland, past and present. *Pest Management Science* 58(6):515–
599 520, doi: 10.1002/ps.491, URL <http://onlinelibrary.wiley.com/doi/10.1002/ps.491/abstract>
- 601 Ranta E, Kaitala V, Lindstrom J, Linden H (1995) Synchrony in Population Dynamics. *Proceedings of the*
602 *Royal Society of London Series B: Biological Sciences* 262(1364):113–118, doi: 10.1098/rspb.1995.0184,
603 URL <http://rspb.royalsocietypublishing.org/content/262/1364/113.abstract>
- 604 Revie CW, Gettinby G, Treasurer JW, Rae GH, Clark N (2002) Temporal, environmental and manage-
605 ment factors influencing the epidemiological patterns of sea lice (*Lepeophtheirus salmonis*) infestations
606 on farmed Atlantic salmon *Salmo salar* in Scotland. *Pest Management Science* 58(6):576–584, URL
607 <http://onlinelibrary.wiley.com/doi/10.1002/ps.476/abstract>
- 608 Revie CW, Gettinby G, Treasurer JW, Wallace C (2003) Identifying epidemiological factors affecting sea
609 lice *Lepeophtheirus salmonis* abundance on Scottish salmon farms using general linear models. *Diseases*
610 *of Aquatic Organisms* 57(1-2):85–95, URL <http://www.int-res.com/abstracts/dao/v57/n1-2/p85-95/>
- 612 Rinaldi S, Candaten M, Casagrandi R (2001) Evidence of peak to peak dynamics in ecology. *Ecology Letters*
613 4:610–617, URL <http://onlinelibrary.wiley.com/doi/10.1046/j.1461-0248.2001.>

- 00273.x/full
- 614 Rogers LA, Peacock SJ, McKenzie P, DeDominicis S, Jones SRM, Chandler P, Foreman MGG, Revie
615 CW, Krkošek M (2013) Modeling parasite dynamics on farmed salmon for precautionary conservation
616 management of wild salmon. PLoS ONE 8(4):e60096, doi: 10.1371/journal.pone.0060096, URL <http://dx.doi.org/10.1371/journal.pone.0060096>
617
618
- 619 Sah P, Paul Salve J, Dey S (2013) Stabilizing biological populations and metapopulations through Adaptive
620 Limiter Control. Journal of theoretical biology 320:113–23, doi: 10.1016/j.jtbi.2012.12.014, URL <http://www.sciencedirect.com/science/article/pii/S002251931200642X>
621
- 622 Samways MJ (1979) Immigration, population growth and mortality of insects and mites on cassava in
623 Brazil. Bulletin of Entomological Research 69(03):491–505, URL <http://dx.doi.org/10.1017/S000748530001899X>
624
- 625 Schaffer WM (1985) Order and chaos in ecological systems. Ecology 66(1):93–106, URL <http://www.esajournals.org/doi/abs/10.2307/1941309>
626
- 627 Silva A (2003) Morphometric variation among sardine (*Sardina pilchardus*) populations from the northeastern
628 Atlantic and the western Mediterranean. ICES Journal of Marine Science 3139(03):1352–1360, doi: 10.
629 1016/S1054, URL <http://icesjms.oxfordjournals.org/content/60/6/1352.short>
- 630 Spratt J (2003) Chaos and time-series analysis. Oxford University Press, URL <http://spratt.physics.wisc.edu/chaostsa/>
631
- 632 Steen H, Ims RA, Sonerud GA, Steen H (1996) Spatial and Temporal Patterns of Small-Rodent Population
633 Dynamics at a Regional Scale. Ecology 77(8):2365–2372, URL <http://www.esajournals.org/doi/abs/10.2307/2265738>
634
- 635 Stien A, Bjørn PA, Heuch PA, Elston DA (2005) Population dynamics of salmon lice *Lepeophtheirus salmonis*
636 on Atlantic salmon and sea trout. Marine Ecology Progress Series 290(Kabata 1979):263–275, doi: 10.3354/
637 meps290263, URL <http://dx.doi.org/10.3354/meps290263>
- 638 Sugihara G, May R, Ye H, Hsieh Ch, Deyle E, Fogarty M, Munch S (2012) Detecting Causal-
639 ity in Complex Ecosystems. Science 338(6106):496–500, doi: 10.1126/science.1227079, URL
640 <http://www.ncbi.nlm.nih.gov/pubmed/22997134><http://www.sciencemag.org/content/338/6106/496.abstract>
641
- 642 Tompkins DM, Carver S, Jones ME, Krkošek M, Skerratt LF (2015) Emerging infectious diseases of wildlife:
643 a critical perspective. Trends in Parasitology 31(4):149–159, doi: 10.1016/j.pt.2015.01.007, URL <http://linkinghub.elsevier.com/retrieve/pii/S1471492215000197>
644
- 645 Van Bael S, Pruett-Jones S (1996) Exponential Population Growth of Monk Parakeets in the United States. The
646 Wilson Bulletin 108(3):584–588, URL <http://www.jstor.org/stable/4163726>
- 647 Walker PJ, Winton JR (2010) Emerging viral diseases of fish and shrimp. Veterinary Research 41(6), doi:
648 10.1051/vetres/2010022

649 A Solution to ODE

650 The solutions to Eq. (1) are:

$$\begin{aligned} u(t) &= f_u(t, u_0, v_0) \\ &= c_1 \exp\left[\frac{r_{uu} + r_{vv} + \alpha}{2}t\right] + c_2 \exp\left[\frac{r_{uu} + r_{vv} - \alpha}{2}t\right] \end{aligned} \quad (\text{A.1})$$

$$\begin{aligned} v(t) &= f_v(t, u_0, v_0) \\ &= c_1 \left(\frac{r_{vv} - r_{uu} + \alpha}{2r_{uv}}\right) \exp\left[\frac{r_{uu} + r_{vv} + \alpha}{2}t\right] + c_2 \left(\frac{r_{vv} - r_{uu} - \alpha}{2r_{uv}}\right) \exp\left[\frac{r_{uu} + r_{vv} - \alpha}{2}t\right], \end{aligned} \quad (\text{A.2})$$

where

$$c_1 = \frac{2r_{uv}v_0 - u_0(r_{vv} - r_{uu} - \alpha)}{2\alpha} \quad (\text{A.3})$$

$$c_2 = \frac{u_0(\alpha + r_{vv} - r_{uu}) - 2r_{uv}v_0}{2\alpha} \quad (\text{A.4})$$

$$\alpha = \sqrt{(r_{uu} - r_{vv})^2 + 4r_{uv}r_{vu}}. \quad (\text{A.5})$$

651 To get the time of the next treatment given the growth rates and initial conditions, we first rearrange Eqs (A.1-A.2). We denote
652 the time of the next treatment of u and v as T_u and T_v , respectively. The equations for T_u and T_v are:

$$\begin{aligned} 2\alpha N_{\max} = \exp\left(\frac{r_{uu} + r_{vv}}{2}T_u\right) &\left[\left(\exp\left(\frac{\alpha}{2}T_u\right) - \exp\left(\frac{-\alpha}{2}T_u\right)\right)(2r_{uv}v_0 + u_0(r_{uu} - r_{vv}))\right. \\ &\left. + u_0\alpha\left(\exp\left(\frac{\alpha}{2}T_u\right) + \exp\left(\frac{-\alpha}{2}T_u\right)\right)\right] \end{aligned} \quad (\text{A.6})$$

$$\begin{aligned} 4\alpha r_{uv} N_{\max} = \exp\left(\frac{r_{uu} + r_{vv}}{2}T_v\right) &[(2r_{uv}v_0(r_{vv} - r_{uu}) + 4u_0r_{vu}r_{uv}) \\ &\left(\exp\left(\frac{\alpha}{2}T_v\right) - \exp\left(\frac{-\alpha}{2}T_v\right)\right) + 2r_{uv}v_0\alpha\left(\exp\left(\frac{\alpha}{2}T_v\right) + \exp\left(\frac{-\alpha}{2}T_v\right)\right)] \end{aligned} \quad (\text{A.7})$$

653 In Eqs (A.6-A.7), T_u and T_v cannot be solved for explicitly, so we used a numerical root finding algorithm to determine T_u and
654 T_v .

655 B Development of return map

656 We used the dynamical system described in Eq. (2) to construct a return map that takes the population density u when v is treated
657 and returns u the next time v is treated. We first consider the scenario where u is not treated in between consecutive treatments of
658 v . We denote the time to the next treatment of v as T_{v0} . In this case, the resulting population density u at the next treatment of v is

$$\phi(u^*) = f_u(T_{v0}, u^*, N_{\min}), \quad (\text{B.1})$$

659 where f_u is the solutions to Eq. (1), given in Appendix A. Next, we consider the case where u is treated once in between treatments
660 of v . This leads to a return map of the form,

$$\phi(u^*) = f_u(T_{v1}, N_{\min}, f_v(T_{u0}, u^*, N_{\min})), \quad (\text{B.2})$$

661 where T_{u0} is the time from the initial treatment of v to the treatment of u and T_{v1} is the subsequent time from the treatment of u
662 to the next treatment of v . These two cases can be combined into a single equation as,

$$\phi(u^*) = \underbrace{H(\tilde{T}_0) f_u(T_{v0}, u^*, N_{\min})}_{u \text{ not treated}} + \underbrace{H(\tilde{T}_1) [1 - H(\tilde{T}_0)] f_u(T_{v1}, N_{\min}, f_v(T_{u0}, u^*, N_{\min}))}_{u \text{ treated once}}. \quad (\text{B.3})$$

663 We can continue in this way to get the equation that includes the possibility for u being treated twice in between treatments of
664 v ,

$$\begin{aligned} \phi(u^*) = & \underbrace{H(\tilde{T}_0) f_u(T_{v0}, u^*, N_{\min})}_{u \text{ not treated}} \\ & + \underbrace{H(\tilde{T}_1) [1 - H(\tilde{T}_0)] f_u(T_{v1}, N_{\min}, f_v(T_{u0}, u^*, N_{\min}))}_{u \text{ treated once}} \\ & + \underbrace{H(\tilde{T}_2) [1 - H(\tilde{T}_1)] f_u(T_{v2}, N_{\min}, f_v(T_{u1}, N_{\min}, f_v(T_{u0}, u^*, N_{\min})))}_{u \text{ treated twice}}. \end{aligned} \quad (\text{B.4})$$

665 By induction, we arrive at the general equation for the return map, given in (3):

$$\phi(u^*) = \underbrace{[H(\tilde{T}_0)] f_u(T_{v0}, u^*, N_{\min})}_{m=0} + \underbrace{\left[\sum_{m=1}^{\infty} H(\tilde{T}_m) \prod_{n=0}^{m-1} [1 - H(\tilde{T}_n)] \right] f_u(T_{vm}, N_{\min}, v_{m-1})}_{m \geq 1}. \quad (\text{B.5})$$

666 C Algorithm describing return map

667 Because Eqs (A.6-A.7) can not be solved for T_u and T_v , model analysis by the return map involved simulating successive treatments
668 until v was treated next. The recursive algorithm we applied to calculate the population density u when v was treated next is:

<pre>function u_next(u, v, R) evaluate T_u(u, v, R) = Tu evaluate T_v(u, v, R) = Tv if (T_u > T_v) then return f_u(T_v, u, v) else v_new = f_v(T_u, u, v) return u_next(Nmin, v_new, R) end if</pre>	<p>Calculate the time to the next treatment of u and the time to the next treatment of v If the time to treatment of v is less, return u when v is treated. Otherwise, u is treated. Calculate v when u is treated and repeat function with new initial values.</p>
---	---

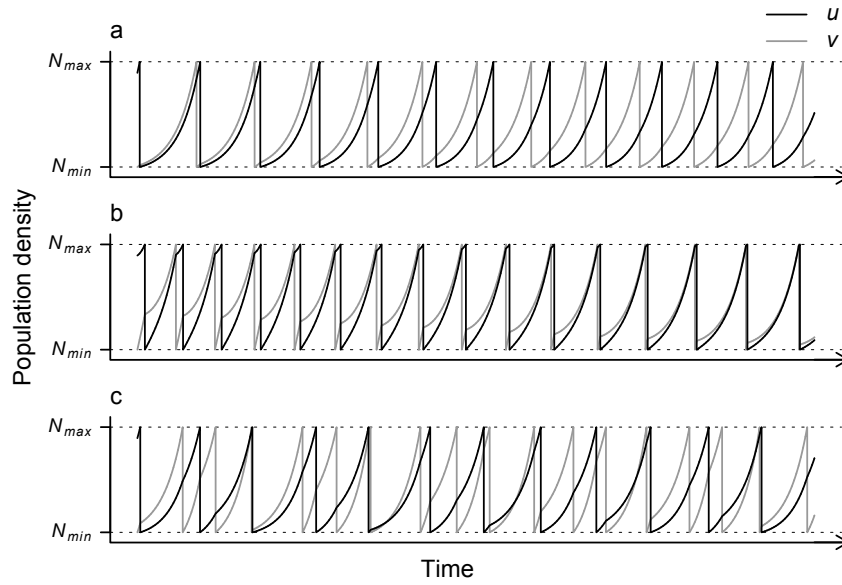


Fig. 1 Three types of behaviour observed were observed for connected populations subject to control: (a) alternating treatments of populations for equal growth rates of the two populations and connectivity less than the internal growth rates ($r_{ij}/r_{ii} = 0.1$), (b) synchrony in the population dynamics between patches for equal growth rates of the two populations and connectivity greater than the internal growth rates ($r_{ij}/r_{ii} = 10$) and (c) apparently chaotic dynamics where the treatment timing was unpredictable for unequal growth rates of the two populations. Initial conditions were $u_0 = 2.7$ (black line) and $v_0 = N_{\min}$ (grey line). The upper and lower horizontal dashed lines indicate the treatment threshold and abundance of parasite immediately after treatment, respectively.

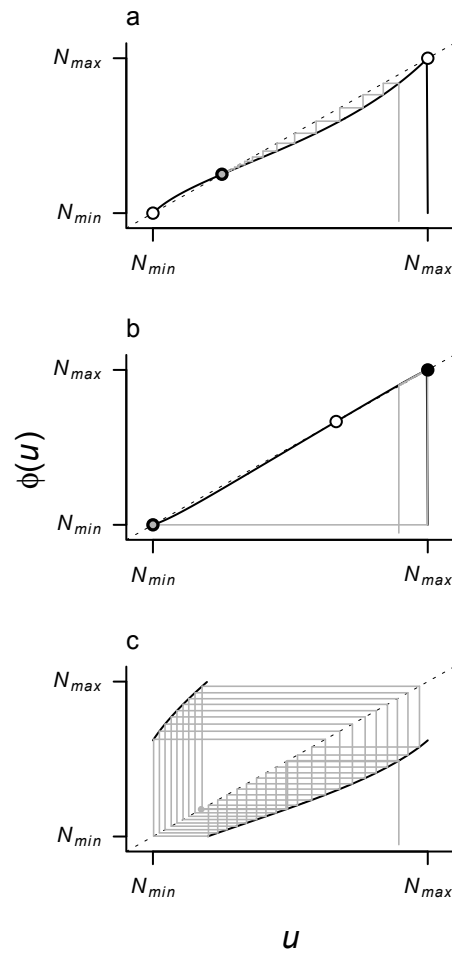


Fig. 2 Return maps for the population density u at re-treatment of v ($\phi(u^*)$) over increasing initial population density, u^* . (a) For low connectivity, there was a stable equilibrium in (N_{min}, N_{max}) (black point) and unstable equilibria at N_{min} and N_{max} (white points). (b) When connectivity was higher than internal growth, there was an unstable equilibrium in (N_{min}, N_{max}) and stable equilibria at N_{min} and N_{max} , and the two populations synchronized. (c) For unequal connectivity, u was treated m or $m + 1$ times before v was treated, yielding a discontinuity in the return map that resulted in cycles. The relative growth rates in each panel correspond to those in Fig. 1. The grey lines show 30 iterations of the return map (i.e., cobwebbing) from $u^* = 2.7$, ending at the grey point).

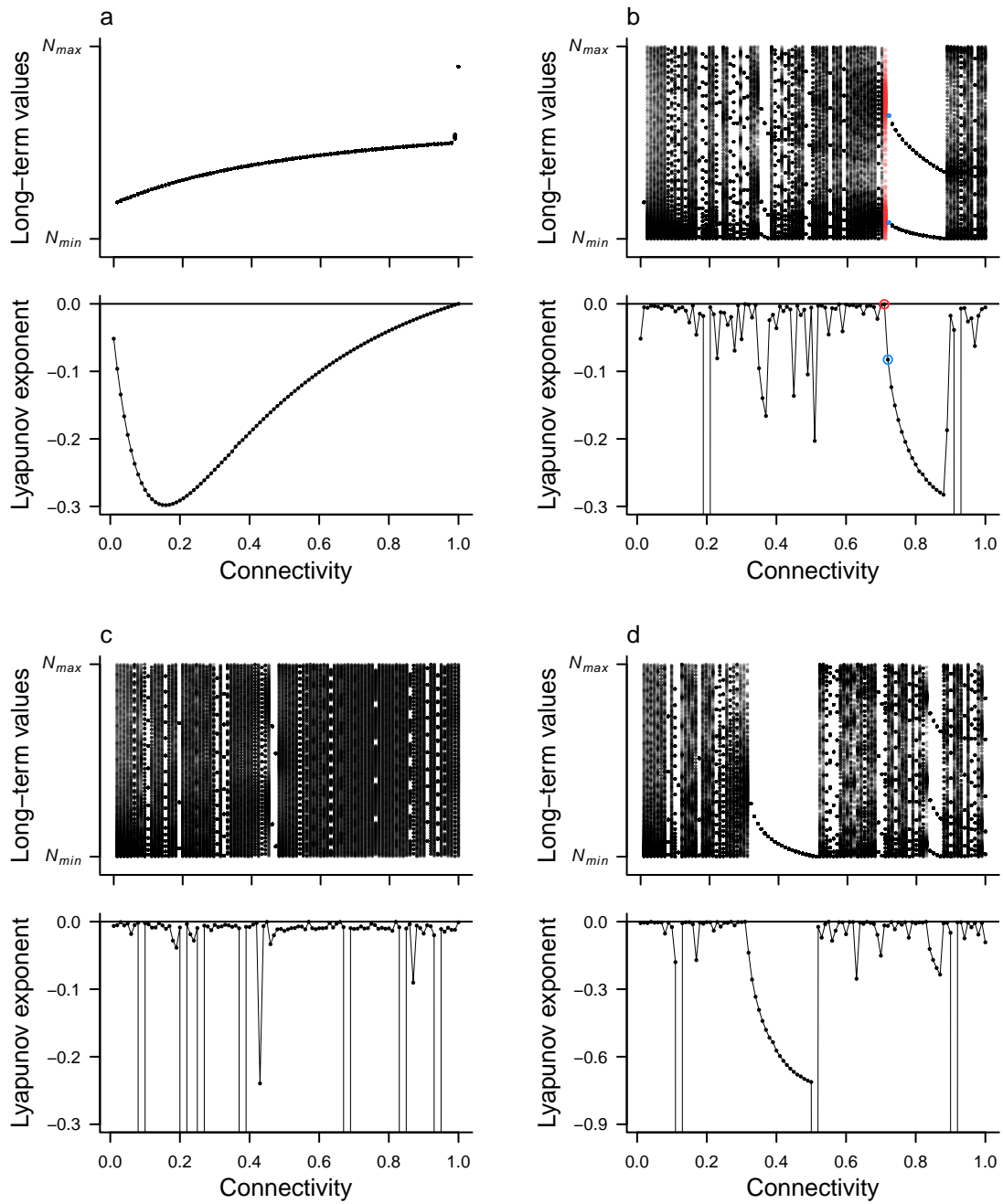


Fig. 3 Long-term values of $\phi(u^*)$ and the Lyapunov exponents λ under four different scenarios for changing connectivity (a-d; scenarios A-D in Table 1). In calculating long-term values, for each value of connectivity we plotted the last 500 of 2000 iterations starting at $u_0^* = 2.7$ (see Fig. S1 for results with other starting values). Red and blue points in (c) indicate the parameter values for stochastic simulations in Fig. 5. Online version in colour.

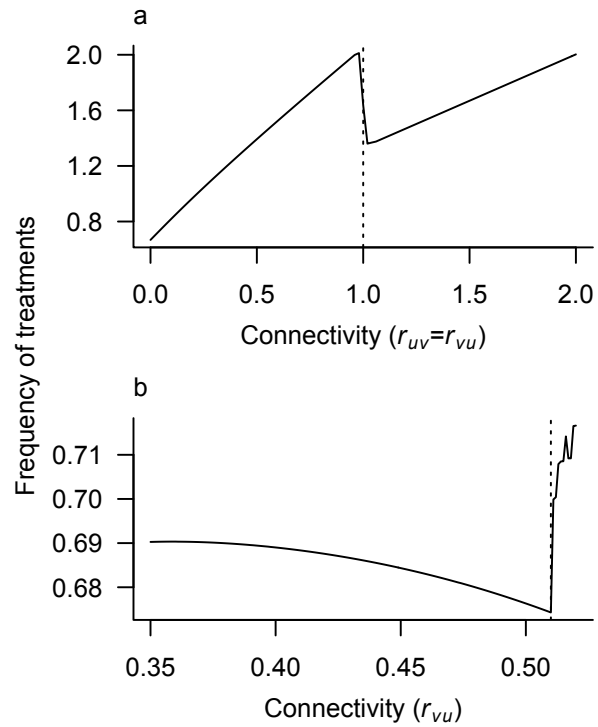


Fig. 4 The frequency of treatments over increasing connectivity. (a) In scenario A, the frequency of treatments drops when the connectivity exceeds internal growth rates (dotted line) and populations become synchronized (Table 2), but rises again as connectivity increases further due to increasing total growth rate. (b) In scenario D, the frequency of treatments declines over the region of phase locking (see Fig. 3d) as the stable point approaches N_{\min} , reducing the impact of the rescue-effect. The minimum frequency of treatments occurs where populations are synchronized at $r_{vu} + r_{vv} = r_{uv} + r_{uu}$ (i.e. $r_{vu} = 0.51$, dotted line; Table 2).

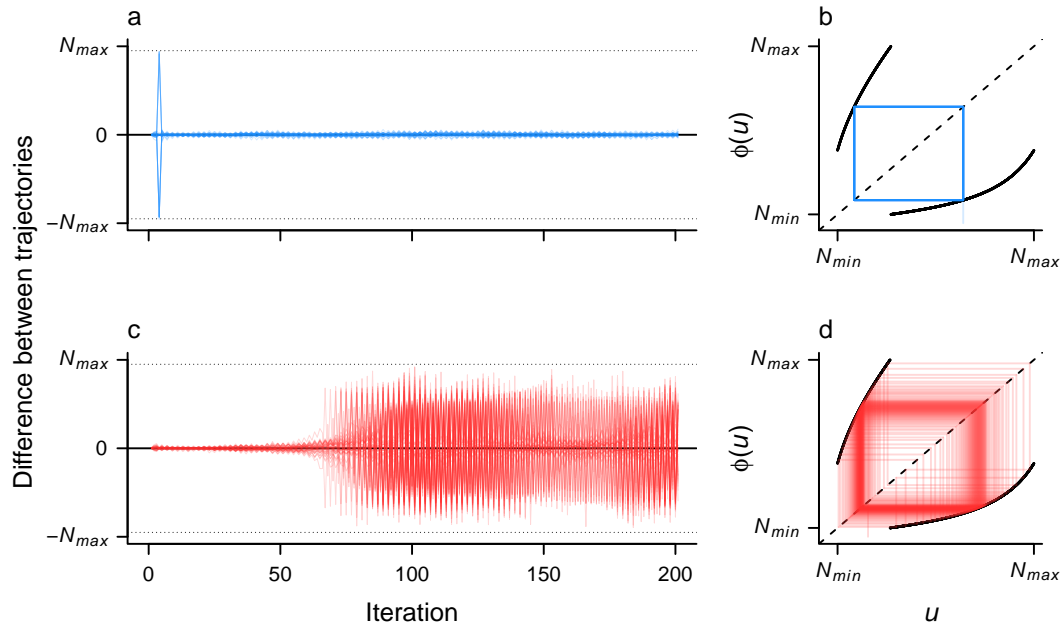


Fig. 5 The effect of stochasticity differed with small changes in parameters. The difference between two trajectories initially separated by ϵ_0 remained small for parameters under which the deterministic model showed periodic dynamics (a), but increased for parameters under which the deterministic model showed quasiperiodic dynamics (c). The corresponding deterministic return maps of the fiducial trajectory for scenario B with $r_{vu} = 0.72$ (b) and $r_{vu} = 0.71$ (d) (see Fig. 3b). Online version in colour.